NAVAL POSTGRADUATE SCHOOL
Monterey, California

THESIS

ASSESSING THE EFFECTS OF MODEL ERROR ON RADAR INFERRED EVAPORATIVE DUCTS

by

Marc C. Eckardt

March 2002

Thesis Advisor:	Kenneth L. Davidson
Second Reader:	L. Ted Rogers

Approved for public release; distribution is unlimited.

Report Documentation Page

Report Date	Report Type	Dates Covered (from... to)
29 Mar 2002	N/A	-

Title and Subtitle Assessing the Effects of Model Error on Radar Inferred Evaporative Ducts	**Contract Number**
	Grant Number
	Program Element Number
Author(s) Eckardt, Marc	**Project Number**
	Task Number
	Work Unit Number
Performing Organization Name(s) and Address(es) Naval Postgradaute School Monterey, California	**Performing Organization Report Number**
Sponsoring/Monitoring Agency Name(s) and Address(es)	**Sponsor/Monitor's Acronym(s)**
	Sponsor/Monitor's Report Number(s)
Distribution/Availability Statement Approved for public release, distribution unlimited	
Supplementary Notes The original document contains color images.	
Abstract	
Subject Terms	
Report Classification unclassified	**Classification of this page** unclassified
Classification of Abstract unclassified	**Limitation of Abstract** UU
Number of Pages 70	

THIS PAGE INTENTIONALLY LEFT BLANK

REPORT DOCUMENTATION PAGE			Form Approved OMB No. 0704-0188
Public reporting burden for this collection of information is estimated to average 1 hour per response, including the time for reviewing instruction, searching existing data sources, gathering and maintaining the data needed, and completing and reviewing the collection of information. Send comments regarding this burden estimate or any other aspect of this collection of information, including suggestions for reducing this burden, to Washington headquarters Services, Directorate for Information Operations and Reports, 1215 Jefferson Davis Highway, Suite 1204, Arlington, VA 22202-4302, and to the Office of Management and Budget, Paperwork Reduction Project (0704-0188) Washington DC 20503.			
1. AGENCY USE ONLY *(Leave blank)*	**2. REPORT DATE** March 2002	**3. REPORT TYPE AND DATES COVERED** Master's Thesis	
4. TITLE AND SUBTITLE: Assessing The Effects Of Model Error On Radar Inferred Evaporative Ducts			**5. FUNDING NUMBERS**
6. AUTHOR(S) Marc C. Eckardt			
7. PERFORMING ORGANIZATION NAME(S) AND ADDRESS(ES) Naval Postgraduate School Monterey, CA 93943-5000			**8. PERFORMING ORGANIZATION REPORT NUMBER**
9. SPONSORING /MONITORING AGENCY NAME(S) AND ADDRESS(ES) Space and Naval Warfare Systems Command (SPAWAR), PMW-155 4301 Pacific Highway, San Diego, CA 92110-3127			**10. SPONSORING/MONITORING AGENCY REPORT NUMBER**
11. SUPPLEMENTARY NOTES The views expressed in this thesis are those of the author and do not reflect the official policy or position of the Department of Defense or the U.S. Government.			
12a. DISTRIBUTION / AVAILABILITY STATEMENT Approved for public release; distribution is unlimited.			**12b. DISTRIBUTION CODE**

13. ABSTRACT ***(maximum 200 words)***

A method for inferring evaporative duct refractivity profiles from radar clutter was introduced by *Rogers et al.* (2000) called Refractivity from Clutter (RFC). Climatological data from three tactical ocean areas of interest were used to investigation the RFC method using a numerical simulation of an S-band radar. The magnitude of the error introduced by inferring a neutrally equivalent refractive profile from one parameter (radar clutter) was compared against the traditional bulk method which calculates the profile based on environmental measurements. A benchmark for the simulated RFC error was determined by applying measurement errors to the simulated environment and by then calculating refractive profiles using the bulk method. Results of the simulation show that the error introduced by the RFC method is comparable to the error caused by measurement errors for the traditional method. The neutral equivalent profile inferred by RFC exhibited slightly increasing error with height and more than twice the error with frequency when applied to X-band propagation. Finally, a method for investigating tactical impacts of using refractive profiles against low flying anti-ship missiles was developed. Results show that the simulated RFC method determined the detection range of several hypothetical missiles within five percent of the actual predicted range.

14. SUBJECT TERMS Refractivity From Clutter (RFC), Radar Propagation, Evaporation Duct			**15. NUMBER OF PAGES** 70
			16. PRICE CODE
17. SECURITY CLASSIFICATION OF REPORT Unclassified	**18. SECURITY CLASSIFICATION OF THIS PAGE** Unclassified	**19. SECURITY CLASSIFICATION OF ABSTRACT** Unclassified	**20. LIMITATION OF ABSTRACT** UL

NSN 7540-01-280-5500 Standard Form 298 (Rev. 2-89)
Prescribed by ANSI Std. 239-18

THIS PAGE INTENTIONALLY LEFT BLANK

Approved for public release; distribution is unlimited.

ASSESSING THE EFFECTS OF MODEL ERROR ON RADAR INFERRED EVAPORATIVE DUCTS

Marc C. Eckardt
Lieutenant Commander, United States Navy
B.S., United States Naval Academy, 1992

Submitted in partial fulfillment of the
requirements for the degree of

MASTER OF SCIENCE IN METEOROLOGY AND PHYSICAL OCEANOGRAPHY

from the

NAVAL POSTGRADUATE SCHOOL
March 2002

Author: Marc C. Eckardt

Approved by: Kenneth L. Davidson
Thesis Advisor

L. Ted Rogers
Thesis Co-Advisor

Carlyle H. Wash
Chairman, Department of Meteorology

THIS PAGE INTENTIONALLY LEFT BLANK

ABSTRACT

A method for inferring evaporative duct refractivity profiles from radar clutter was introduced by *Rogers et al.* (2000) called Refractivity from Clutter (RFC). Climatological data from three tactical ocean areas of interest were used to investigation the RFC method using a numerical simulation of an S-band radar. The magnitude of the error introduced by inferring a neutrally equivalent refractive profile from one parameter (radar clutter) was compared against the traditional bulk method which calculates the profile based on environmental measurements. A benchmark for the simulated RFC error was determined by applying measurement errors to the simulated environment and by then calculating refractive profiles using the bulk method. Results of the simulation show that the error introduced by the RFC method is comparable to the error caused by measurement errors for the traditional method. The neutral equivalent profile inferred by RFC exhibited slightly increasing error with height and more than twice the error with frequency when applied to X-band propagation. Finally, a method for investigating tactical impacts of using refractive profiles against low flying anti-ship missiles was developed. Results show that the simulated RFC method determined the detection range of several hypothetical missiles within five percent of the actual predicted range.

THIS PAGE INTENTIONALLY LEFT BLANK

TABLE OF CONTENTS

LIST OF FIGURES

THIS PAGE INTENTIONALLY LEFT BLANK

LIST OF TABLES

THIS PAGE INTENTIONALLY LEFT BLANK

ACKNOWLEDGMENTS

To Heather for giving me patience and to Devin Grace for giving me perspective.

THIS PAGE INTENTIONALLY LEFT BLANK

EXECUTIVE SUMMARY

The requirement to have an accurate and up-to-date knowledge of refractive conditions in the immediately above the sea exists in the Navy. Current methods to meet this requirement are either labor intensive, inaccurate, untimely, or provide generalizations of the atmospheric conditions vice specifics. A method for inferring evaporative duct refractivity profiles from radar clutter was introduced by *Rogers et al.* (2000) called Refractivity from Clutter (RFC). RFC provides a more timely and automated way of providing refractive information to the radar operator and tactical decision makers. The process of inferring the refractive properties of the atmosphere from the existing radar clutter introduces some errors. Similarly, measuring the environment and calculating the refractive profile using established methods also has unavoidable errors. The goal of this thesis was to evaluate the cost of using the RFC method to infer the refractive profile vice using the traditional method.

Climatological data from three tactical ocean areas of interest were used to investigation the RFC approach using a numerical simulation of an S-band radar. The magnitude of the error introduced by inferring a neutrally equivalent refractive profile from one parameter (radar clutter) was compared against the traditional bulk method which calculates the profile based on environmental measurements. A benchmark for the simulated RFC error was determined by applying measurement errors to the simulated environment and by then calculating refractive profiles using the bulk method.

Results of the simulation show that the error introduced by the RFC method is comparable to the error caused by measurement errors for the traditional method. The neutral equivalent profile inferred by RFC exhibited slightly increasing error with height and more than twice the error with frequency when applied to X-band propagation. Finally, a method for investigating tactical impacts of using refractive profiles against low flying anti-ship missiles was developed. Results show that the simulated RFC method determined the detection range of several hypothetical missiles within five percent of the actual predicted range.

I. INTRODUCTION

A. ATMOSPHERIC EFFECTS ON ELECTROMAGNETIC PROPAGATION

The impacts that the atmosphere has on electromagnetic propagation is widely known and well studied. However, the practical determination of the responsible atmospheric properties and tactical application of this knowledge doesn't seem to meet the requirements within the military and specifically the surface navy. Significant efforts are in progress to both educate and aid the war-fighter on the refractive effects of radar propagation and the tactical adjustments needed to exploit or mitigate those impacts. In particular, low flying anti-ship missiles are of high concern and one of the marine near-surface atmosphere dominant features, the evaporation duct, has a significant impact on the detection and engagement of these threats. In some cases, engagements cannot be achieved without the enhanced propagation caused by the existence of an evaporation duct. However, without the near-continuous and timely knowledge of their existence and properties, adjustments to ship sensors cannot be made to achieve satisfactory results.

Traditional methods to determine the refractive conditions caused by evaporation ducting include measuring certain atmospheric parameters and applying theory to determine the refractive profile of the boundary layer. While these systems are in development, radar operators currently use the Aegis "slide-rule" or series of "thumb-rules" to determine if ducting conditions exist and if so, how to adjust the radar to take advantage of increased surface ranges. A new method, called Refractivity from Clutter (RFC), infers the evaporative duct profile "through the sensor" by using the radar clutter as the sole parameter in lieu of measuring specific atmospheric parameters. Recent testing in conjunction with the Tactical Environmental Processor (TEP) onboard two Aegis cruisers showed encouraging results while eliminating much of the manual procedures associated with traditional methods. However, the RFC method is relatively unknown and not fully understood as to its own accuracy and limitations. This thesis attempts to explore some of these areas and determine the errors associated with inferring an evaporative duct described using a single parameter.

THIS PAGE INTENTIONALLY LEFT BLANK

II. BACKGROUND AND THEORY

A. REFRACTIVITY AND EVAPORATIVE DUCTS

Refraction has a significant effect on the performance of ship radars due to the radar frequency and to airflow properties immediately above the sea. The refraction of electromagnetic energy is mainly due to vertical gradients of the atmospheric pressure, temperature and water vapor content with the latter being the most important adjacent to the sea surface. For energy in the range of naval radars, the index of refraction (n) is modified to highlight subtle changes that have significant impacts:

$$N = (n-1)*10^6 \tag{1}$$

It is the change of N with height that is needed to determine the refractive effects of the atmosphere; thus it is the change of pressure, temperature and water vapor that is required to calculate the refractivity:

$$\frac{dN}{dz} = C_1 \frac{dP}{dz} + C_2 \frac{dT}{dz} + C_3 \frac{de}{dz} \tag{2}$$

A trapping or ducting condition exist when dN/dz < -0.157 (m^{-1}) and therefore when specifically discussing ducts, it is useful to define a 'modified' index of refraction (M) such that a negative M gradient indicates ducting conditions:

$$M = N_z + 157z \tag{3}$$

Evaporative ducts are the term given to the condition that occurs in the atmospheric boundary layer over water due to large humidity gradients immediately above the surface and are limited in vertical extent. Mixing in the boundary layer creates a relatively shallow zone where humidity drops off from one hundred percent to a lower uniform value above the boundary layer. It is this decrease of water vapor in conjunction with temperature increases or decreases that create the evaporative duct. For some applications, only the height of the evaporation duct is required; however, for tactical implications the entire gradient profile is required not merely the height where M is a minimum.

B. GRADIENT PROFILES

1. The Profile (Bulk) Approach

Bulk models are useful because they provide a way of determining the surface-layer profiles from a single-height and surface measurement. This 'profile (bulk) approach' for the evaporation duct determines the change of *M* with height, referred to as the *M* profile, based on the bulk-determined pressure (P), temperature (T) and water vapor (q) profiles. Monin-Obukhov Similarity (MOS) theory provides a way of relating the profiles to surface fluxes, which then relate the bulk measurements at the surface as the basis of the profile. MOS theory assumes that the environment is horizontally homogeneous and stationary with the turbulent fluxes of momentum, sensible heat and latent heat to be constant with height (within the surface layer). The flux-profile relationship for any conservative quantity (*S*) is given by equation (4) and the stability function by equation (5).

$$\frac{\partial S}{\partial z} = \frac{S_*}{kz}\Phi_S\left(\frac{z}{L}\right) \tag{4}$$

$$\xi = \frac{z}{L} = \frac{zkg(T_* + 0.61Tq_*)}{T_v u_*^2} \tag{5}$$

Atmospheric scaling parameters from the surface layer model are defined by flux quantities:

$$u_* = \sqrt{(-\overline{w'u'})} \tag{6}$$

$$T_* = -\frac{\overline{w'T'}}{u_*} \tag{7}$$

$$q_* = -\frac{\overline{w'q'}}{u_*}Z \tag{8}$$

Expanding (7) and (8) by the stability function (5) into measurable quantities yields:

$$T_* = \frac{(T_z - T_0)k}{\ln(\frac{z}{z_{oT}}) - \psi_T(\xi)} \tag{9}$$

$$q_* = \frac{(q_z - q_0)k}{\ln(\frac{z}{z_{oq}}) - \psi_q(\xi)} \tag{10}$$

2. The Stability Dependent Profile

An approach by *Liu et. al* (1979), known as LKB, was used to derive a bulk method to estimate the gradient of *M*:

$$M(z) = 77.6\frac{P}{T} + 3.73*10^5\frac{e}{T^2} + 0.157z \tag{11}$$

The LKB model is a bulk surface-layer scaling model that uses a MOS approach to calculate the near-surface *M* profile. *Frederickson et al.* (2000) adapted the LKB model in a manner similar to that used by *Babin et al.* (1997), to create the Naval Postgraduate School version of the LKB model (referred to as NPS-LKB). Both of these approaches are based on the general expression for the gradient of a conservative quantity, equation (4), integrated from z_0 to some height z:

$$S(z) = S_0 + \frac{S_*}{k}\left[\ln\frac{z}{z_0} - \psi_S\left(\frac{z}{L}\right)\right] \tag{12}$$

The NPS-LKB model uses integrated profile functions. It improves the convergence of the model in highly stable, low wind conditions and also uses a new form for the thermal roughness Reynolds number (R_θ). In contrast to the model suggested by *Babin et al.* (1997), the NPS-LKB model uses the full three-term equation for refractivity (*N*) is order to more completely account for subtle changes caused by water vapor which in certain stable cases can significantly change the profile.

3. The Neutral Evaporation Duct Profile

The neutral profile approach is also based on the integrated function for a scalar, equation (12). Assumptions by the *Jeske* (1971, 1973) and *Paulus* (1985) approach is

that the potential refractivity (N_p) is the conservative quantity and when converted to M units yields the integration:

$$M(z) = M_0 + 0.13z - 0.13\frac{\delta}{\varphi\left(\frac{\delta}{L}\right)}\left[\ln\frac{z}{z_0} - \psi\left(\frac{z}{L}\right)\right] \tag{13}$$

The evaporation duct height (δ) is defined in this approach as the height at which the gradient of potential refractivity is equal to –0.13 (where dM/dz = 0). The neutral evaporation duct approach uses equation (13) and assumes a neutrally stable environment such that the stability dependent functions are removed ($\varphi \rightarrow 1$ and $\psi \rightarrow 0$) resulting in an M profile that is determined from a single parameter (δ):

$$M(z) = M_0 + 0.13z - 0.13\delta\left[\ln\frac{z}{z_0}\right] \tag{14}$$

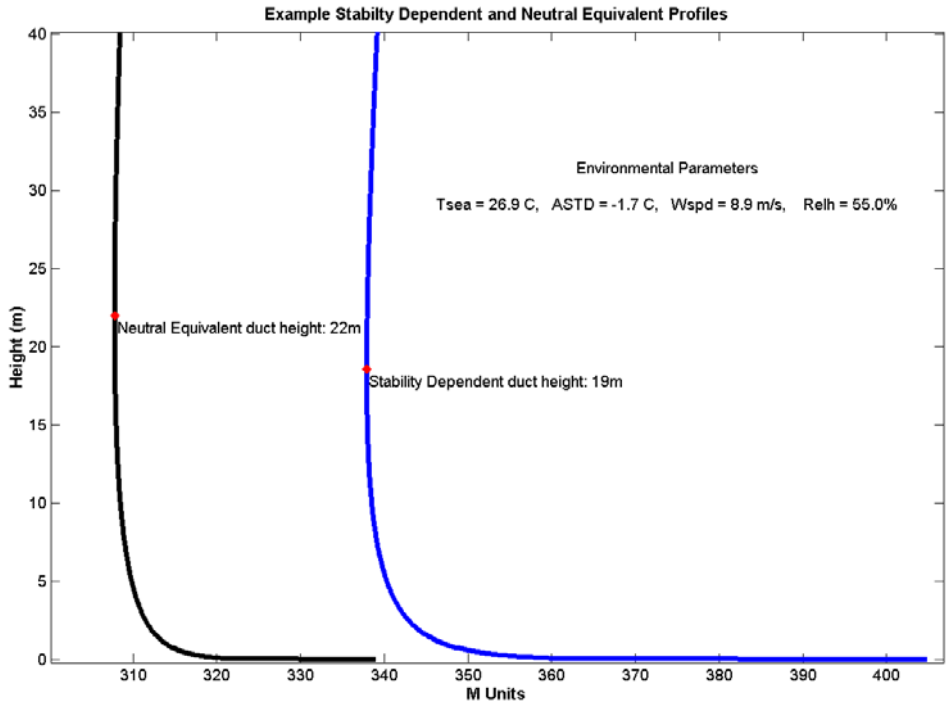

Figure 1. Stability Dependent and Neutral Equivalent Profiles

Figure (1) shows a comparison of a stability dependent profile (blue curve) and corresponding neutral equivalent profile (black curve) inferred via the RFC method. Note the differences in the profiles, specifically the large gradient at the surface for the stability dependent profile and slightly different slope above the duct height (red dot). Subtle differences such as these can make more of a difference in the propagation of radar waves than the height of the evaporation duct does.

4. The Neutral Sub-Refractive Profile

Similar to the neutral evaporation duct equation (14), an equation for sub-refractive (where dN/dz = 0) conditions can be derived under neutral conditions where the gradient of potential refractivity is equal to 0.024:

$$M(z) = M_0 + 0.13z + 0.024\varsigma\left[\ln\frac{z}{z_0}\right] \tag{15}$$

C. REFRACTIVITY FROM CLUTTER (RFC)

1. Introduction

Rogers et al. (2000) proposed the inference of evaporation duct heights from radar sea clutter. Previous modeling studies indicated that the falloff of sea clutter as a function of range was an increasing function of the evaporation duct height (*Pappert et al.* 1992). Results from testing showed a strong correlation between radar inferred duct heights and those calculated from bulk measurements.

2. Method

The RFC method averages the clutter power return of a radar from an inner radius r_i to some outer radius r_f (5-50km in the above case) and subtracts the mean value (referred to as the mean-removed average). This slope is compared against a library of neutral profiles calculated from equation (14) with duct heights from δ=0 to δ=40. The library consists of 41 propagation mean-removed loss curves, as predicted by a propagation model at the height of one meter for each profile. The RFC method matches the observed clutter power return with the neutral profile that has the smallest mean-

removed root-mean-square average. In essence the neutral profile with the closest slope to the observed clutter power return becomes the match and is deemed the "neutral-equivalent" profile since it is the profile that best represents the observed propagation at one meter.

3. Operational Testing

RFC was tested in conjunction with the Tactical Environmental Processor (TEP) onboard two Aegis ships as a means of providing real time automated refractive conditions to the radar operators for tactical purposes. This setup used radar return from the AN/SPY-1B radar operating near the S-band of 3000 MHz. Results from this testing showed that for unstable conditions, the RFC method was comparable to the bulk method and more accurate that the bulk method for stable conditions (when wind speeds were greater than five knots).

D. RFC CONCERNS AND THESIS MOTIVATION

New techniques that require less effort on the part of the user are normally well received under the condition that the system works well in all circumstances. Of primary concern is the application of the RFC method to tactical decisions. The RFC estimate of refractivity corresponds to the neutral evaporation duct that best explains the observed clutter, which is at the height of zero meters. The true refractivity profile is (in general) stability dependent and cannot be fully characterized by the neutral profile. So the question is what costs there are associated with tactically applying this neutrally equivalent profile to a higher height where anti-ship missiles fly. Additionally, since not all radar systems operate in the S-band, whether or not the evaporation duct profiles inferred at the S-band frequency can be used to accurately predict the propagation at a higher frequency like 1 GHz (X-band) is also of interest. Finally, if these issues can be answered, a baseline for 'normal' and / or acceptable error needs to be established. The goal of this thesis is to address the issue of model errors associated with the RFC evaporation duct algorithm through the use of numerical simulations and identify a benchmark for assessing the cost of the model error.

III. THE RFC SIMULATION

A. SCOPE

The RFC evaporation duct algorithm simulations focus on quantifying the impact of the model error, associated with the neutral assumption, in an attempt to address concerns raised in section II.D. In addition to model error, the performance of the RFC evaporation duct algorithm could be degraded by the horizontal variability of radar clutter, radar artifacts, quality control and minimum wind speed limitations (no clutter). Because these simulations do not account for these other sources of error, the simulations do not address the overall performance of the RFC evaporation duct algorithm; they can only address whether or not model error has a significant impact on its performance.

The basic RFC method is reproduced using S-band propagation with errors determined for specific heights of concern where anti-ship missiles normally fly. These profiles are then re-used in the X-band to determine if inferred profiles can be used at higher frequencies. Then, as a benchmark to compare the RFC model error against, each neutral equivalent profile is compared against a profile calculated by the bulk method using normal errors associated with measuring environmental parameters. Other potential errors using this traditional method, including the horizontal variability of the environmental parameters, errors in the stability dependent model itself and wind speed envelopes associated with the SMOOS(R) system, are not investigated. Thus, as is the case with the simulations of the RFC evaporation duct algorithm, these simulations do not address the overall performance of using in situ measurements for evaporation duct characterization. Rather, they only address the impact of expected measurement errors on the system performance.

B. RFC SIMULATION COMPONENTS

To the extent possible, the selection of components that make up the RFC simulation were based on current and /or future US Navy programs and models (MORIAH, SEAWASP, SMOOS(R) and TEP). The selections were of the database, the models for surface layer refractivity, the propagation model, and the measurement uncertainty. Aspects of the selections are described in the following sections.

1. Selected Climatological Database

The three ocean areas of concern addressed in the RFC simulation were: the Persian Gulf, the Arabian Sea, and the South China Sea. Climatologies for these areas were taken from the Global Marine Climatic Atlas (GMCA) provided by the Fleet Numerical Oceanography and Meteorology Detachment, Asheville, North Carolina (FNMOD det Asheville). The GMCA is derived from the Comprehensive Ocean and Atmosphere Data Set (COADS), distributed by the National Center for Atmospheric Research (NCAR), and was primarily collected by surface ships from 1854-1995. The climatic database for this simulation was limited to a thirty-year span covering 1965-1995 within a specified grid box for each area. At the completion of each model run, the predicted duct heights for each area were compared against the Ducting Climatology Summary (DCS) database within the respective Marsden grid.

2. Selected Neutrally Stable Model

Rogers and *Paulus* (1996) proposed a neutral evaporation duct model using the *Jeske* / *Paulus* approach which yield equation (14). A similar process is used by *Paulus* (2000) to describe a neutral sub-refractive model yields equation (15).

3. Selected Stability Dependent Model

Several stability dependent models exist that could be used with the RFC simulation. The *Jeske* / *Paulus* approach has some difficulties in stable conditions, as documented by *Babin et al.* (1997) and though once used in the Integrated Refractive Effects Prediction System (IREPS), is not used in this simulation other than providing the neutral equivalent equations discussed above. A more complex bulk model was introduced by *Liu, Katsaros, and Businger* (1979), known as the LKB model, and is now widely used in the meteorology 'air-sea interaction' scientific community. *Frederickson et al*. (2000) adapted the LKB model with an MOS flux-profile approach to determine the near-surface *M* profile more accurately.

It is speculated that either model could produce relatively similar results because in this simulation the RFC step is independent of the bulk derived *M* profile. However, though these models were investigated for completeness, the final choice of which stability dependent model to use was solely determined by which model is being used in prototype systems like SMOOS(R) and TEP. Further, the NPS-LKB model has now become the model used in the Advanced Refractive Effects Prediction System (AREPS).

4. Selected Propagation Model

The original paper by *Rogers et al.* (2000) used the Terrain Parabolic Equation Model (TPEM) to predict electromagnetic propagation. Since then, IREPS was merged with TPEM to become AREPS, now the US Navy standard for refractive programs. AREPS uses the Advanced Propagation Model (APM) to calculate propagation loss using a number of different user defined parameters. The APM is a hybrid model consisting of four sub-models: flat earth, ray optics, extended optics, and split-step parabolic equation (PE) model. Like the choice of the stability dependent model, APM was used solely because it is in use on surface combatants and the goal of the RFC simulation is to reproduce as much of reality as possible. It should be noted that parabolic equation modeling is a reasonably mature technology with the various models (TEMPER, RPO, etc.) providing similar results at S-band (see, *Paulus* 1995).

5. Selected Measurement Uncertainty / Errors

This simulation attempts to provide a benchmark for assessing the cost of the model error of RFC by determining what the error of the traditional bulk-method approach would be given the unavoidable random measurement errors. Measurement error threshold values, defined as 90% of the time, of the MORIAH / SMOOS(R) system were taken from a draft copy of the Operational Requirements Document, Table 1: System Performance Parameters (summarized in table 1). *Sadanaga* (1999) reported that during an evaluation period of a prototype MORIAH system, only air temperature and relative humidity met ORD threshold requirements. However, for the purpose of this simulation, it is assumed that these threshold levels will eventually be achieved and after consulting with both the Space and Naval Warfare Systems Center (SPAWAR)

Propagation Division and the Johns Hopkins University, Applied Physics Laboratory (JHU/APL), threshold values were interpreted as representing the absolute maximum error of a given sensor with zero bias and a three standard deviation spread. It should be noted that these assumed error distributions correspond to assuming that the air-sea temperature difference (ASTD) is known within ± 0.23°C of its true value. With regard to the goodness of the in situ measurements, this is a generous assumption.

Parameter	Threshold Value	Mean	Standard Deviation
Sea Surface Temperature	± 0.5 °C	$\mu = 0$	$3\sigma = 0.50$ (C)
Air Temperature	± 0.5 °C	$\mu = 0$	$3\sigma = 0.50$ (C)
Wind Speed	± 1.0 kt	$\mu = 0$	$3\sigma = 0.51$ (m/s)
Relative Humidity	± 3.0 %	$\mu = 0$	$3\sigma = 3.00$ (%)
Sea Level Pressure	± 1.0 mb	$\mu = 0$	$3\sigma = 1.00$ (mb)

Table 1. Interpretation of SMOOS(R) System Performance Parameters

C. IDENTIFIED LIMITATIONS IN THE RFC SIMULATION

Due to the choice of model components and assumptions in their application, the RFC simulation has known definite limits. However, these limitations are not believed to significantly hinder an adequate investigation of the RFC method.

These limitations include but are not limited to the following, with regard to model applications:

1. Neutral Equivalent Model

There are limitations because the RFC approach was formulated on the basis of the Neutral Equivalent Model. The original paper on the RFC method (*Rogers et al.* 2000) did not address sub-refractive cases. However, given a library of representative profiles, there is no reason to expect that the RFC method can't match sub-refractive conditions in the same manner as when there are evaporative ducting conditions. The expression used for the neutrally stable case under sub-refractive conditions is a very basic approach and at times can limit the effectiveness of the RFC step since only a limited number of library profiles were created. This is believed to merely limit the

results of this simulation and not the overall effectiveness of RFC since a more thorough sub-refractive model could positively influence the overall effectiveness of RFC.

2. Stability Dependent Model

A further limitation is when stability affects are based on a model predicted versus observed conditions. For the purposes of this simulation, the NPS-LKB model is assumed to be a perfect model that accurately represents the true refractive conditions of the atmosphere for a given set of surface measured parameters. Additionally, not all actual climatology-derived datasets can yield a calculated *M* profile because certain combinations of surface parameters break the assumptions of the NPS-LKB model. In some cases, the stability model produces an unrealistic profile based on limitations on the scaling near-surface properties above the sea for all climatological regimes.

3. Propagation Model

Similar to the need to describe the surface-layer with a stability dependent model, the need to describe propagation effect with a model, the APM, is a limitation. It is assumed for the simulation that APM / AREPS produces a correct representation of what the radar clutter is expected to be at one meter. Many of the advanced features available through AREPS are turned off in this simulation and occasionally an *M* profile, generated by the NPS-LKB model, crashes the APM. In some simulation runs, such as with the Persian Gulf database, up to fifteen percent of the calculated *M* profiles crash the propagation model. The cause of these crashes, whether it is with the input file or with the program itself, is being investigated but tend to be related to the type of refractivity profile. Profiles that crash the APM have one of three conditions:

1) A minimum *M* value at the surface,
2) a minimum *M* value at the top of the layer (100m), or
3) two inflection points in the *M* profile.

a. Minimum M Values at the Surface

The profiles had minimum *M* values at the surface are sub-refractive cases and are routinely exhibited in nature; thus in order to keep these cases, a near-standard gradient was added to the top of the profile (0.13 *M* units per meter). The resultant profile does not change the propagation effects within the first 100 meters since the standard profile is sub-refractive by nature. Of note, the neutral equivalent profile for sub-refractive conditions did not crash the model and thus the cause of these crashes is still being looked at. One possibility is that it is related to the profile slopes and / or the maximum height of the profile.

b. Minimum M Values at 100 Meters

The *M* profiles in the second condition where the minimum values are at the top of the layer cannot be used because it is errant to imply conditions above 100 meters without any additional information. Some of the environmental datasets were rerun through the NPS-LKB model with the 100m height limit moved to 200m and more often than not, the height of duct was between 100 and 200 meters. Thus to apply the same standard *M* profile to these cases as used in the sub-refractive cases would actually change the results. To ensure that APM crashes do not crash the entire simulation, these profiles are coded to skip the entire process and start a new iteration (new profile).

Additionally, there is some question as to the validity of duct heights in excess of 100 meters. Assumptions by MOS theory apply only in the surface layer which is the lowest 10% of the turbulent boundary layer. This is generally between 10 and 200 meters and so the theory begins to break down under some stable conditions where the duct height is not well defined. Moreover, the DCS database (duct height climatology) rarely has duct heights in excess of 80 meters. For these reasons, it is not believed that the exclusion of these profiles significantly changes the results of the simulation; however, since all of these cases are under stable conditions, the final ratio of successful stable to unstable profiles is slightly skewed from the climatology and thus there is a possibility that the errors calculated for the stable and unstable cases are also skewed.

c. Two Inflection Points in the M *Profile*

Cases where the NPS-LKB model generate an M profile with two inflection points are extremely rare (less than 0.05 percent) and arguably are not physical. The exclusion of these cases does not impact the results and like the profiles above, the simulation is coded such that these profiles are skipped and a new iteration started.

4. The RFC Simulation Method

The RFC method as implemented in TEP performs a clutter-power-averaging step that helps smooth errors produced by inconsistent sea clutter (incident angles on swell and grazing angles). This simulation uses only one bearing to represent the clutter-power-averaging step and assumes horizontal homogeneity of the surrounding environment. This may be a safe assumption in the open ocean but clearly has limitations when operating in littoral areas such as the three areas investigated here.

D. SIMULATION FLOWPATH

Each simulation consists of 5000 iterations through the model with each iteration using a different environmental dataset randomly generated from the climatology database for the specified area. The objective of running the model through 5000 iterations is so that an accurate representation of statistics related to the climatology is produced. Early attempts to recreate the climatic conditions using only 1000 iterations did not adequately represent the climate statistics while runs with 10,000 iterations did not appear to represent statistics related to the climatic conditions any better than 5000 iterations.

1. Step 1: Generate an *M* Profile

An individual iteration first involves generating a random sample of the environment based on the climate. MATLAB performs this step by generating a random number based on a Guassian distribution curve defined by the climatological statistics. Since the sea surface temperature and air temperature are not completely independent from one another, the air-sea temperature difference (ASTD) field is used to generate the

air temperature once the sea-surface temperature has been created. This was also done to ensure that the ASTD field was accurately represented since it is the stability of the boundary layer that most influences that shape of the *M* profile. Each randomly created dataset is run through a quality control routine to ensure that the generated values for each parameter are realistic and do not fall out of the bounds of the original statistics. (For example, the random number generator of MATLAB could produce a relative humidity value of greater than 100% or a wind speed less that 0 knots.)

Once a set of environmental parameters has been created, the dataset is entered into the NPS-LKB model to produce an *M* profile. The NPS-LKB model setup ingests sea-surface temperature, air temperature, wind speed, relative humidity and sea-level pressure – all measured at a specific (hard coded) height. The output of the model is an *M* profile from 0 to 100 meters in 0.1 meter increments. Iterations that cannot produce an *M* profile are thrown out and a new dataset is generated. Profiles that do produce *M* profiles have a near standard atmosphere *M* profile of 1000 meters added to the tope of the calculated 100 meter layer (0.13 per meter). This step does not affect the propagation effects of the lower 100-meter layer but helps ensure that each profile will successfully run in the APM (discussed in section III.C.3).

Of note, the generated environmental dataset and subsequent *M* profile are assumed to exact depictions of the atmosphere. It is this Stability Dependent (SD) profile that is used as 'truth' when generating and comparing errors.

2. Step 2: Calculate the S-Band Propagation Loss

The SD profile is then entered into the APM in order to produce a propagation loss matrix in decibels (dB) from 0 to 100 meters in one-meter increments and from a range of one to fifty kilometers in one-kilometer increments. This creates a 101 by 50 grid that represents the propagation loss of a simulated AN/SPY-1B radar operating at a height of twenty meters in the S-Band (3000 MHz nominal value). Like before, this loss matrix is assumed to be a perfect representation of the true atmosphere and the loss at one meter the expected clutter power loss a radar would have.

3. Step 3: Determine the Neutral Equivalent Profile

In an operational environment the only known value is the clutter power loss that is averaged azimuthally around the ship from five to fifty kilometers due to other interfering effects close into the ship. This simulation uses the predicted propagation loss of the SD profile at one meter to represent the clutter power loss and finds the Neutral Equivalent (NE) profile based on the procedure described in section II.C.2. Once the NE profile has been determined, this profile is entered into the APM and a neutral equivalent loss matrix is generated.

4. Step 4: Calculate the 'Scientific' Error

In order to help address the issues raised by the RFC method, each simulation requires a 'height of concern' that represents the height at which a low flying anti-ship missile could operate. Due to the classification of these values, nominal 'ballpark' values were chosen that best represent the general area of operation for these missiles; however; an error tolerance of plus or minus three meters is applied to simulate the tactical variations and impacts of weather on flight paths.

The loss matrix of the NE profile is subtracted from the loss matrix of the SD profile to produce a loss-difference matrix for S-Band propagation. Using the 'height of concern' and three-meter tolerance, the Root-Mean-Square (RMS) error at each grid point is calculated and the total RMS calculated for the individual iteration. (For example: if the height of concern is fifteen meters, the RMS error is calculated for all grid points between twelve to eighteen meters.) The RMS error is referred to as the 'scientific' error in order to distinguish from another error calculated using a non-standard method.

5. Step 5: Apply the Profiles to X-Band

One of the concerns of RFC is whether a profile inferred by the clutter power loss in the S-Band can be used to accurately predict the propagation of other frequencies, specifically higher frequencies in the X-Band. (X-Band is of importance because it is near the frequency of other radars and tactical systems.) This step uses the existing SD

and NE profiles and reruns the propagation model at a frequency of one gigahertz. A difference matrix is then produced and an RMS error calculated.

6. Step 6: Calculate the 'Tactical' Error

a. Discussion

To provide a qualitative assessment of the potential tactical impacts of inferring a refractive profile through the radar vice measuring it in some fashion, a 'tactical' error method was developed. Due to the classification of the Aegis system, attempts to use the radar equation, developed by *Barton* (1988) with subsequent RFC applications by *Gerstoft et al.* (2001), in order to calculate a range of maximum detection based on the refractive profile proved to difficult and inaccurate. Thus using 'nominal' values of established detection ranges for the Aegis system, the tactical impact of the NE was investigated. The purpose here is to at least pursue an error method that is easily understandable and transferable to radar operators. Routinely on surface ships, 'new' methods are introduced that claim good results but daily operations by shipboard personnel prove otherwise. It would be helpful to inform the tactical watch standers that under certain testing criteria, the RFC system predicted that actual detection range within 'Y' percent. This type of comparison is difficult because in order to pass scrutiny it must be scientifically sound yet not so much so that the results do not translate to those without the academic background. The mechanism developed here is admittedly in error yet still provides some insight into the tactical implications of radar inferred duct heights.

b. Implementation

In addition to a 'height of concern', each simulation run has a given detection range that the Aegis system would detect a target in a standard atmosphere (again actual values are classified). The neutral evaporation duct profile at zero meters is a near standard atmosphere and thus is used as a baseline to determine the dB level at which detection occurs based on the given detection range. The assumption here is that the detection of a target is noise limited and thus once the propagation loss is less than that of the dB level, detection occurs. The SD profile is used as truth such that if the propagation loss curve crosses the 'detection threshold dB level', this represents the

actual detection range. The same process is done for the NE profile and the two detection ranges are compared for accuracy using a simple error calculated based on the percent difference between the two ranges. It is important to highlight that this method is being accomplished for qualitative purposes only in order to make general comments on what the tactical impacts could be for a given method. Also, this type of comparison is only valid in S-Band since X-Band is not used for detection; no reasonable comparison is available at the higher frequency.

7. Step 7: Repeat the Process Using Measurement Errors

The entire process is repeated for each iteration starting after step 2 using measurement errors applied to the original SD profile. This is accomplished by using generating a random error based on the specifications of the sensors. Once applied to the original environmental dataset, the NPS-LKB model is run again to produce a 'Modified Stability Dependent' profile (referred to as 'mod-SD'). The mod-SD profile is run through the APM at both S-Band and X-Band and the same errors are calculated thus providing the benchmark for comparative purposes.

THIS PAGE INTENTIONALLY LEFT BLANK

IV. SIMULATION RUNS

A. INTRODUCTION

1. Model Inputs

Each simulation run pertains to an RFC evaluation with regard to a climatological database region (for area of responsibility (AOR) applicability), a target height (for the RMS error) and a nominal detection range of that target (for detection range errors). To test a wide spectrum of conditions yet still attempt to have the simulation evaluate realistic conditions, the following combinations were chosen for the simulation:

Target Height – Detection Range	Persian Gulf	Arabian Sea	South China Sea
5 m – 10 nm	PG.5.10	AS.5.10	SCS.5.10
15 m – 10 nm	PG.15.10	AS.15.10	SCS.15.10
30 m – 18 nm	PG.30.18	AS.30.18	SCS.30.18

Table 2. Combinations of Inputs for RFC Simulation Runs

2. Model Conversions for Simulations

Although units in the simulation models are normally referenced with metric units, distance units in the surface navy are routinely discussed in nautical miles and not meters or kilometers; thus both the input and tactical output displays use nautical miles. Moreover, wind speeds are commonly referred to in knots vice meters per second and so a conversion is also made. In every case except for the detection range determination, all conversions are carried through with sufficient decimals to ensure that a rounding error does not affect the simulation results.

3. Simulation with Sub-Refractive Profiles

As discussed, initial RFC testing-based formulation (*Rogers et al.* 2000) did not include a method to generate a neutrally equivalent profile under sub-refractive

conditions mainly because sub-refractive conditions were not observed during the experiment. As a carryover, initial model runs did not account for sub-refractive conditions which in extreme cases accounted for over ten percent of all iterations. As previously discussed, a simple model was developed to expand the original library of neutral evaporative duct profiles to include neutral sub-refractive profiles as well. Upon close examination of the sub-refractive profiles generated by the simulation, there is some skepticism as to whether the stability dependent profiles are realistic or not, in this case. A change of 50 *M* units in 100 meters is considered extreme in most cases (with the exception being right at the boundary interface); however many of the sub-refractive profiles created by the simulation have changes of over 150 *M* units in 100 meters as shown in figure (2). The S-band RMS error for the profile in figure (2) was 26.57 dB using the RFC method which clearly skews the final statistics.

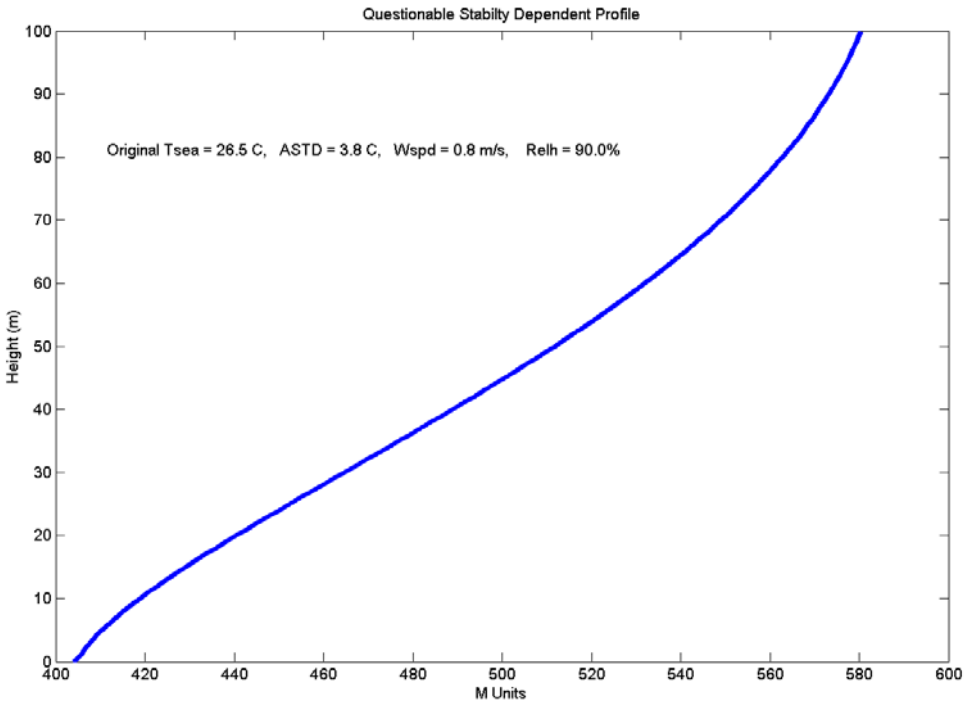

Figure 2. Questionable Stability Dependent Profile

Due to sub-refractive modeling issues and the questions raised by such extreme *M* profiles, each simulation calculates a set of RMS errors based on all the iterations and

another set of errors that exclude all of the sub-refractive cases. This is done for comparative purposes to help understand the error introduced by the sub-refractive profiles. Without sufficient background knowledge and objective analysis of these cases, there is no basis on which to subjectively throw out certain cases while keeping others that seem to fit conventional wisdom. However, since the RFC method matches the slopes in the falloff of clutter power, the model should be able to generate a neutral profile given an adequate library to choose from regardless of whether the stability dependent profiles are realistic or not.

It is noted that the sub-refractive model implemented within RFC for the simulations is almost certainly sub-optimal. That implies that the simulation results using the sub-refractive model are sub-optimal as well; i.e., it may be possible to obtain better results when an improved sub-refractive model is implemented.

B. PERSIAN GULF

1. Climatology

Table (3) lists the statistics taken from the GMCA from 1965 to 1995, for observations over all months and over all hours, in the Persian Gulf. Data was centered at 26.83 North, 51.66 East and encompasses about a one degree box of historical observations. The warm temperatures of the Persian Gulf are such that high water vapor values are expected at the near-surface boundary. This, combined with little mechanical mixing (wind speeds less than 6 m/s) and relative humidity values less than 75% on average, means that a large water vapor gradient is expected which could influence tactical systems year round. Though the average air-sea temperature is almost zero, indicating near-neutral conditions, the Persian Gulf has a seasonal variation not well represented by this dataset that favors stable conditions in the summer months and unstable conditions in the winter months.

	Observations	Mean	Min	Max	Std Dev
Wind Speed (m/s)	102274	5.57	0.00	22.10	3.44
Air Temp (C)	111921	26.19	6.20	42.00	5.93
Sea Temp (C)	87737	26.47	12.20	37.90	4.95
Air-Sea Temp Diff (C)	80196	-0.03	-5.00	12.70	2.49
Sea Level Pressure (mb)	102363	1010.02	987.10	1031.20	7.90
Relative Humidity (%)	77797	72.96	11.50	100.00	13.01

Table 3. Persian Gulf Climatology bases on GMCA

2. PG.5.10 RMS Error

a. Without Sub-Refractive Cases

RMS Error (dB) from 2 – 8 m					
		NE vs. SD		Mod-SD vs. SD	
		Mean	Std	Mean	Std
S band	Total	0.59	0.33	0.75	1.31
	Stable	0.58	0.44	1.42	1.94
	Unstable	0.60	0.25	0.38	0.44
X band	Total	4.13	2.34	1.71	2.10
	Stable	3.74	2.34	2.80	2.93
	Unstable	4.36	2.31	1.11	1.05

Table 4. PG.5.10 RMS Error Without Sub-Refractive Cases

b. With Sub-Refractive Cases

RMS Error (dB) from 2 – 8 m					
		NE vs. SD		Mod-SD vs. SD	
		Mean	Std	Mean	Std
S band	Total	0.95	1.87	1.01	1.88
	Stable	1.46	2.84	1.98	2.67
	Unstable	0.60	0.25	0.38	0.44
X band	Total	4.67	3.44	2.10	2.76
	Stable	5.15	4.59	3.59	3.71
	Unstable	4.35	2.31	1.11	1.05

Table 5. PG.5.10 RMS Error With Sub-Refractive Cases

c. Discussion

The simulated RFC method statistically out performs the traditional method with measurement errors, when sub-refractive cases are not included, displaying a small RMS error and little spread in S band with little to no stability dependence. When sub-refractive cases are considered, the two methods are comparable and a stability dependence is evident as the stable cases have a much larger mean and standard deviation. In all cases, the X-band error is greater in the simulation RFC method; however, not evident in the numbers is that in most cases, both methods provide an adequate visual representation of X-band propagation regardless of the statistical error.

3. PG.15.10 RMS Error

a. Without Sub-Refractive Cases

RMS Error (dB) from 12 – 18 m					
		NE vs. SD		Mod-SD vs. SD	
		Mean	Std	Mean	Std
S band	Total	0.86	0.40	0.68	1.18
	Stable	0.79	0.52	1.29	1.76
	Unstable	0.91	0.29	0.33	0.32
X band	Total	3.21	1.46	1.55	1.82
	Stable	2.75	1.65	2.55	2.60
	Unstable	3.47	1.26	1.00	0.73

Table 6. PG.15.10 RMS Error Without Sub-Refractive Cases

b. With Sub-Refractive Cases

RMS Error (dB) from 12 – 18 m					
		NE vs. SD		Mod-SD vs. SD	
		Mean	Std	Mean	Std
S band	Total	1.24	2.22	0.91	1.74
	Stable	1.73	3.41	1.80	2.50
	Unstable	0.90	0.30	0.33	0.32
X band	Total	3.70	2.84	1.94	2.66
	Stable	4.03	4.17	3.38	3.69
	Unstable	3.47	1.26	1.00	0.73

Table 7. PG.15.10 RMS Error With Sub-Refractive Cases

c. Discussion

The simulated RFC method in the 15-meter case is comparable to the traditional method but with a more mixed statistical error set. In the first run, the S-band error has a higher mean but a much lower spread while in the second run, both the mean and spread are slightly higher than the stability dependent method. Similar to the 5 meter cases, the X-band error, shown in figure (3), is higher but still provides an adequate representation of the predicted propagation. The figure shows 4 pairs of graphs grouped vertically with the top row representing the RFC method and the bottom row the traditional method with measurement errors. The blue line in the left set of graphs is the stability dependent profile used as ground truth for this particular iteration. The black line in the upper left graph is the neutral equivalent profile while the green line in the lower left graph is the modified stability dependent profile. The second set of graphs are identical and represent the propagation based on the stability dependent profile. The third set represents the propagation based on either the RFC profile or the modified profile accordingly. The right set of graphs are the differences between the actual and the predicted propagation values for each particular method.

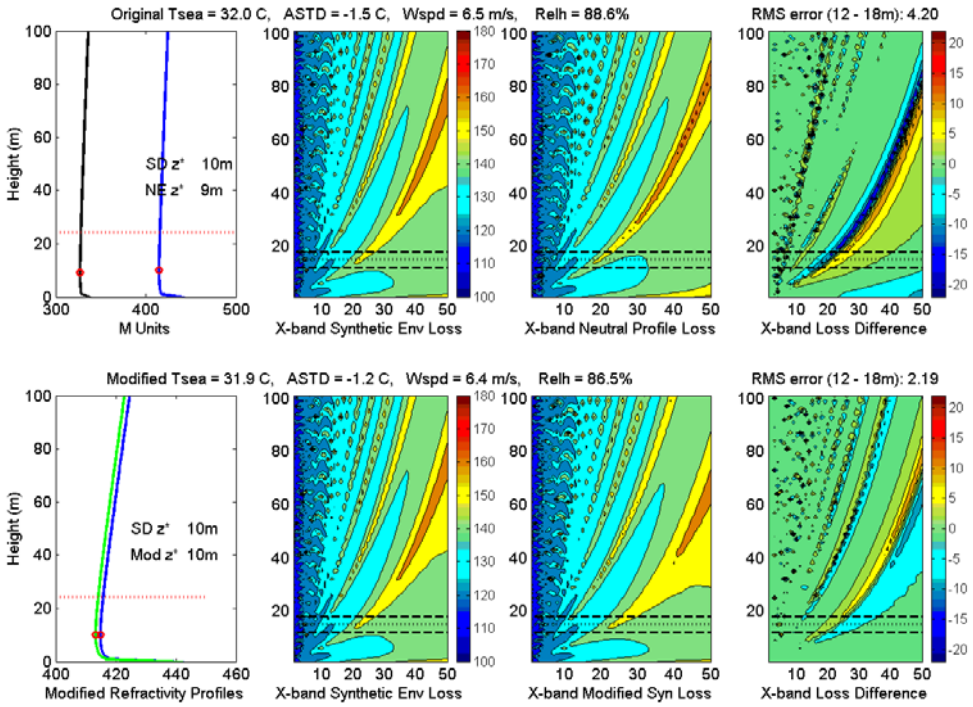

Figure 3. X-band Propagation for Simulated RFC Methods

4. PG.30.18 RMS Error

a. Without Sub-Refractive Cases

RMS Error (dB) from 27 - 33 m					
		NE vs. SD		Mod-SD vs. SD	
		Mean	Std	Mean	Std
S band	Total	1.04	0.55	0.68	1.03
	Stable	1.02	0.71	1.28	1.50
	Unstable	1.04	0.43	0.34	0.28
X band	Total	3.15	1.37	2.10	1.89
	Stable	2.64	1.44	3.30	2.48
	Unstable	3.45	1.23	1.41	0.90

Table 8. PG.30.18 RMS Error Without Sub-Refractive Cases

b. With Sub-Refractive Cases

RMS Error (dB) from 27 – 33 m					
		NE vs. SD		Mod-SD vs. SD	
		Mean	Std	Mean	Std
S band	Total	1.38	2.26	0.94	1.79
	Stable	1.86	3.45	1.84	2.57
	Unstable	1.04	0.43	0.34	0.28
X band	Total	3.53	2.49	2.47	2.69
	Stable	3.65	3.60	4.05	3.56
	Unstable	3.45	1.23	1.41	0.90

Table 9. PG.30.18 RMS Error With Sub-Refractive Cases

c. Discussion

This case in particular performed the poorest of all the simulated RFC model runs at S-band. This is most likely due to the influence the height of the duct has on propagation. In many stable cases, the actual height of the duct was higher than the inferred neutral equivalent profile and since propagation is more influenced by a higher duct, the simulated RFC method did not predict the conditions as well. This can be seen visually in the loss-difference matrixes as the simulated RFC method has the first major side-lobe slightly off in respect to position, resulting in a narrow area of larger errors. In figure (4), the predicted placement of the side-lobe for the RFC method is slightly off resulting in more error at the 30 meter level (top right graph). If the height of interest had

been 5 meters, the error would not be as large but at 30 meters. Of interest, the bottom set of graphs shows that the measured method had placement errors as well.

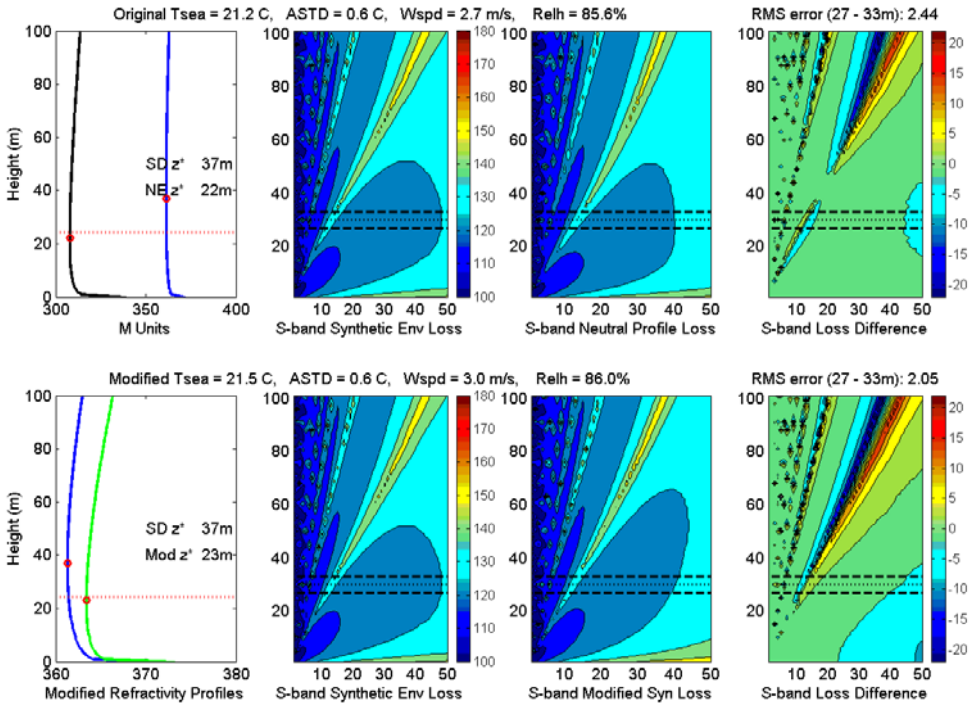

Figure 4. PG.30.18 Example of Side-Lobe Placement Error

The general trend from 5 meters up to 30 meters has been an increase in the S-band error and a slight decrease in the X-band error for the simulated RFC method while the traditional method more independent of height. This result is expected and not as dramatic as originally anticipated in that the RFC method generates the neutral equivalent profile at 1 meter and thus error should be expected as the height increases. Another noticeable trend is that model runs that exclude the sub-refractive profiles do not display a stability dependence while the runs that include them do display a stability dependence. Meaning, the amount of error is directly influenced by the air-sea temperature difference (ASTD); i.e., when conditions are unstable (ASTD < 0 such that the air temperature is cooler than the sea temperature), the error is smaller than when conditions are stable (ASTD > 0).

5. Detection Range Errors

Table (10) lists the tactical errors as determined by the predicted detection range method previously described. Though these numbers should not be used as ground truth, due to the determination method, they do indicate that tactically both methods are comparable and work well such that the predicted detection ranges are normally within at least 10% of the actual detection range. What is not shown by the number is that large RMS error values do not necessarily equate to larger detection range errors.

Detection Range Error (%) for Persian Gulf				
	NE vs. SD		Mod-SD vs. SD	
	Mean	Std	Mean	Std
PG.5.10	-0.24	2.45	-0.37	7.63
PG.15.10	-1.07	7.66	-0.02	5.92
PG.30.18	-1.79	3.84	0.08	3.66

Table 10. Persian Gulf Detection Range Errors

C. ARABIAN SEA

1. Climatology

Table 3 lists the statistics taken from the GMCA from 1965 to 1995, for observations over all months and over all hours, in the Arabian Sea. Data was centered at 21.98 North, 63.35 East and encompasses about a two degree box of historical observations. This body of water is very similar to the Persian Gulf but with slightly stronger winds, a larger spread in the air-sea temperature difference and not as strong of a seasonal variation with respect to when stable or unstable conditions occur. This area is more influenced by the monsoon cycle than the Persian Gulf, which is somewhat protected by terrain, and thus different enough from the Persian Gulf to warrant investigation.

	Observations	Mean	Min	Max	Std Dev
Wind Speed (m/s)	117021	6.12	0.00	25.70	3.72
Air Temp (C)	120896	26.34	15.50	37.00	2.58
Sea Temp (C)	110571	26.71	17.00	35.10	2.16
Air-Sea Temp Diff (C)	106597	-0.41	-10.10	10.30	1.88
Sea Level Pressure (mb)	118508	1009.74	986.80	1028.40	6.61
Relative Humidity (%)	105818	77.10	10.30	100.00	12.06

Table 11. Arabian Sea Climatology bases on GMCA

2. AS.5.10 RMS Error

a. Without Sub-Refractive Cases

RMS Error (dB) from 2 – 8 m					
		NE vs. SD		Mod-SD vs. SD	
		Mean	Std	Mean	Std
S band	Total	0.56	0.31	0.74	1.31
	Stable	0.51	0.39	1.41	2.05
	Unstable	0.58	0.25	0.42	0.46
X band	Total	3.85	2.29	1.62	1.84
	Stable	3.33	2.35	2.63	2.59
	Unstable	4.11	2.21	1.14	1.04

Table 12. AS.5.10 RMS Error Without Sub-Refractive Cases

b. With Sub-Refractive Cases

RMS Error (dB) from 2 – 8 m					
		NE vs. SD		Mod-SD vs. SD	
		Mean	Std	Mean	Std
S band	Total	0.74	1.17	0.91	1.64
	Stable	1.03	1.87	1.80	2.45
	Unstable	0.58	0.25	0.43	0.46
X band	Total	4.18	2.98	1.91	2.39
	Stable	4.31	3.98	3.28	3.34
	Unstable	4.11	2.21	1.15	1.06

Table 13. AS.5.10 RMS Error With Sub-Refractive Cases

c. Discussion

Similar to the Persian Gulf 5-meter case, the simulated RFC method statistically out performs the traditional method with measurement errors in the S-band.

The X-band propagation is just the opposite with the error twice as large for the radar inferred evaporative ducts. However, the overall shape and profile is more similar to the actual profile than it is dissimilar and thus still useful for generalization purposes.

3. AS.15.10 RMS Error

a. Without Sub-Refractive Cases

RMS Error (dB) from 12 – 18 m					
		NE vs. SD		Mod-SD vs. SD	
		Mean	Std	Mean	Std
S band	Total	0.82	0.37	0.66	1.04
	Stable	0.70	0.46	1.24	1.60
	Unstable	0.88	0.29	0.38	0.41
X band	Total	3.05	1.43	1.54	1.61
	Stable	2.38	1.51	2.44	2.32
	Unstable	3.38	1.26	1.11	0.86

Table 14. AS.15.10 RMS Error Without Sub-Refractive Cases

b. With Sub-Refractive Cases

RMS Error (dB) from 12 – 18 m					
		NE vs. SD		Mod-SD vs. SD	
		Mean	Std	Mean	Std
S band	Total	1.04	1.51	0.84	1.51
	Stable	1.33	2.44	1.66	2.26
	Unstable	0.88	0.29	0.38	0.41
X band	Total	3.39	2.41	1.85	2.31
	Stable	3.41	3.64	3.18	3.29
	Unstable	3.38	1.26	1.12	0.88

Table 15. AS.15.10 RMS Error With Sub-Refractive Cases

c. Discussion

These cases are also very similar to the Persian Gulf cases with the same general trends as exhibited before: the S-band error of the simulated RFC method has increased from 5 meters to 15 meters while the X-band error has decreased. With or without the sub-refractive cases, the two methods are again comparable.

4. AS.30.18 RMS Error

a. Without Sub-Refractive Cases

RMS Error (dB) from 27 - 33 m					
		NE vs. SD		Mod-SD vs. SD	
		Mean	Std	Mean	Std
S band	Total	0.93	0.48	0.64	0.98
	Stable	0.85	0.58	1.24	1.52
	Unstable	0.97	0.42	0.36	0.31
X band	Total	3.00	1.36	2.09	1.84
	Stable	2.32	1.40	3.27	2.57
	Unstable	3.31	1.23	1.54	0.98

Table 16. AS.30.18 RMS Error Without Sub-Refractive Cases

b. With Sub-Refractive Cases

RMS Error (dB) from 27 – 33 m					
		NE vs. SD		Mod-SD vs. SD	
		Mean	Std	Mean	Std
S band	Total	1.08	1.29	0.82	1.58
	Stable	1.30	2.10	1.69	2.44
	Unstable	0.97	0.42	0.37	0.31
X band	Total	3.23	2.00	2.35	2.47
	Stable	3.06	2.95	3.88	3.50
	Unstable	3.31	1.23	1.54	0.98

Table 17. AS.30.18 RMS Error With Sub-Refractive Cases

c. Discussion

Unlike the Persian Gulf 30-meter case, which was statistically the worst, this 30 meter case is slightly better than the Arabian Sea 15-meter case. The overall trends observed in the Persian Gulf model runs is still evident and the overall results of the two geographic areas very similar. In hind-sight, the Arabian Sea may be too similar to the Persian Gulf such that the results of these three cases add little to no new information to that already observed other than to reinforce that the simulated RFC model error is comparable to the traditional method, with measurement errors, of determining duct profiles.

5. Detection Range Errors

The results here are slightly better than the Persian Gulf cases and in all cases the margin of error is better for the simulated RFC method than that of the traditional method. Again, it is tactically encouraging that large RMS errors do not translate into large tactical errors as shown by relatively low detection range errors for both methods.

Detection Range Error (%) for Arabian Sea				
	NE vs. SD		Mod-SD vs. SD	
	Mean	Std	Mean	Std
AS.5.10	-0.16	2.27	-0.26	7.31
AS.15.10	-0.81	4.78	-0.09	5.97
AS.30.18	-1.74	2.87	-0.02	3.64

Table 18. Arabian Sea Gulf Detection Range Errors

D. SOUTH CHINA SEA

1. Climatology

Table 3 lists the statistics taken from the GMCA from 1965 to 1995, for observations over all months and over all hours, in the South China Sea. Data was centered at 15.23 North, 115.27 East and encompasses about a two degree box of historical observations. Surprisingly, on average this area has higher wind speeds, higher air temperatures, higher sea temperatures and higher relative humidity values, all with less variation than either the Persian Gulf or the Arabian Sea. Due to these higher values, this climate has the potential to produce a wider spread of ducting conditions.

	Observations	Mean	Min	Max	Std Dev
Wind Speed (m/s)	114677	6.78	0.00	25.70	3.95
Air Temp (C)	116302	27.86	18.00	36.10	2.22
Sea Temp (C)	110096	28.27	19.00	34.00	1.89
Air-Sea Temp Diff (C)	107585	-0.31	-8.30	7.50	1.84
Sea Level Pressure (mb)	115588	1010.38	992.90	1026.60	3.96
Relative Humidity (%)	101275	81.63	46.20	100.00	7.36

Table 19. South China Sea Climatology bases on GMCA

2. SCS.5.10 RMS Error

a. Without Sub-Refractive Cases

RMS Error (dB) from 2 – 8 m					
		NE vs. SD		Mod-SD vs. SD	
		Mean	Std	Mean	Std
S band	Total	0.50	0.32	0.84	1.24
	Stable	0.46	0.41	1.48	1.78
	Unstable	0.53	0.24	0.48	0.53
X band	Total	3.41	2.25	1.75	1.93
	Stable	2.80	2.28	2.68	2.62
	Unstable	3.75	2.16	1.23	1.10

Table 20. SCS.5.10 RMS Error Without Sub-Refractive Cases

b. With Sub-Refractive Cases

RMS Error (dB) from 2 – 8 m					
		NE vs. SD		Mod-SD vs. SD	
		Mean	Std	Mean	Std
S band	Total	0.63	0.93	0.98	1.59
	Stable	0.79	1.45	1.79	2.25
	Unstable	0.53	0.24	0.48	0.53
X band	Total	3.64	2.72	2.00	2.52
	Stable	3.47	3.43	3.25	3.47
	Unstable	3.75	2.16	1.23	1.10

Table 21. SCS.5.10 RMS Error With Sub-Refractive Cases

c. Discussion

The South China Sea 5-meter case shows similar results to the other 5-meter cases but is statistically the best case for the S-band simulated RFC method and the worst case for the modified stability dependent method. A visual inspection of both the raw data and some of the actual profiles indicates that the traditional method was much more error prone on the stable cases as small measurement errors made significant differences in the shape of the profile, resulting in larger RMS errors (figure (5)).

3. SCS.15.10 RMS Error

a. Without Sub-Refractive Cases

RMS Error (dB) from 12 – 18 m					
		NE vs. SD		Mod-SD vs. SD	
		Mean	Std	Mean	Std
S band	Total	0.76	0.40	0.73	1.14
	Stable	0.65	0.50	1.35	1.72
	Unstable	0.82	0.32	0.41	0.37
X band	Total	2.83	1.51	1.71	1.78
	Stable	2.22	1.70	2.71	2.53
	Unstable	3.15	1.29	1.19	0.85

Table 22. SCS.15.10 RMS Error Without Sub-Refractive Cases

b. With Sub-Refractive Cases

RMS Error (dB) from 12 – 18 m					
		NE vs. SD		Mod-SD vs. SD	
		Mean	Std	Mean	Std
S band	Total	0.94	1.28	0.89	1.57
	Stable	1.12	2.03	1.71	2.32
	Unstable	0.82	0.32	0.41	0.37
X band	Total	3.12	2.29	1.98	2.40
	Stable	3.06	3.34	3.33	3.38
	Unstable	3.15	1.29	1.19	0.85

Table 23. SCS.15.10 RMS Error With Sub-Refractive Cases

c. Discussion

These sets of model runs is best described as average since the results here are almost identical to the composite errors presented later. Results here are also very similar to the 15-meter counterparts with the same recurring trends observed in all the previous cases.

4. SCS.30.18 RMS Error

a. Without Sub-Refractive Cases

RMS Error (dB) from 27 - 33 m					
		NE vs. SD		Mod-SD vs. SD	
		Mean	Std	Mean	Std
S band	Total	0.82	0.45	0.72	0.96
	Stable	0.76	0.57	1.27	1.37
	Unstable	0.85	0.36	0.41	0.32
X band	Total	2.77	1.38	2.39	1.96
	Stable	2.16	1.43	3.59	2.50
	Unstable	3.11	1.23	1.71	1.10

Table 24. SCS.30.18 RMS Error Without Sub-Refractive Cases

b. With Sub-Refractive Cases

RMS Error (dB) from 27 – 33 m					
		NE vs. SD		Mod-SD vs. SD	
		Mean	Std	Mean	Std
S band	Total	0.94	1.02	0.85	1.27
	Stable	1.08	1.56	1.54	1.79
	Unstable	0.84	0.36	0.41	0.32
X band	Total	2.96	1.86	2.59	2.32
	Stable	2.73	2.53	3.97	2.97
	Unstable	3.11	1.23	1.72	1.10

Table 25. SCS.30.18 RMS Error With Sub-Refractive Cases

c. Discussion

This set of runs was statistically the best at 30 meters for both methods; average errors are less than 1 decibel in S-band and less than 3 decibels in X-band. Otherwise, these runs are also very similar to their 30-meter counterparts and results reinforce the already established observations that show the error of inferring evaporative duct heights is comparable to that of the traditional method with measurement errors.

5. Detection Range Errors

Comparing individual basins, the South China Sea dataset provided the best results for the detection range errors using the simulated RFC method. The traditional method did not fair as well but were still comparable.

Detection Range Error (%) for South China Sea				
	NE vs. SD		Mod-SD vs. SD	
	Mean	Std	Mean	Std
SCS.5.10	-0.35	2.15	-0.15	7.02
SCS.15.10	-0.53	2.91	-0.07	4.89
SCS.30.18	-1.52	2.72	-0.01	3.69

Table 26. South China Sea Detection Range Errors

E. COMPOSITE ERRORS

Composite errors were calculated by a simple average of all nine simulations, with and without the sub-refractive cases for the RMS errors. Numbers confirm previous discussions: the two methods are comparable at S-band and error increases when the profiles are used with higher frequencies (X-band). Detection range errors are also similar and show that for the simulated RFC method, the calculated ranges are within 5% of the actual predicted value for one standard deviation or within 10% for two standard deviations. In other words, over 85% of the cases were accurately predicted within 10% of the actual detection range (as determined by the Stability Dependent profile).

Composite Error For All Cases				
	NE vs. SD		Mod-SD vs. SD	
	Mean	Std	Mean	Std
S band without sub-refractive cases	0.76 dB	0.40 dB	0.72 dB	1.13 dB
S band with sub-refractive cases	0.99 dB	1.51 dB	0.91 dB	1.62 dB
X band without sub-refractive cases	3.07 dB	1.81 dB	1.83 dB	1.86 dB
X band with sub-refractive cases	3.60 dB	2.56 dB	2.13 dB	2.50 dB
Detection Range Error	-0.91 %	3.52 %	-0.10 %	5.53 %

Table 27. Composite Errors For All Simulation Runs

THIS PAGE INTENTIONALLY LEFT BLANK

V. DISCUSSION OF SIMULATION RESULTS

A. STABILITY DEPENDENCE

The stability dependence of the modified stability dependent profiles is obvious regardless of height, frequency or inclusion of sub-refractive profiles. In every case, the stable profiles have at least twice the error of the unstable profiles and in extreme cases have five-to-six times as much error. This dependence is expected and demonstrates the sensitivity of measured parameters when conditions are stable; specifically, small errors in either sea surface temperature, air temperature or wind speed can significantly impact the accuracy of the bulk-formula derived duct profile. Figure (5) shows an example of such a case. The lower left graph shows the stability dependent profile in blue and the modified stability dependent profile in green (with errors). This dramatic change was caused by only a 0.1°C change in ASTD, 0.3 m/s change in wind speed and 0.1% change in relative humidity. The resulting difference in the predicted propagation of an S-band radar is shown in the bottom right graph.

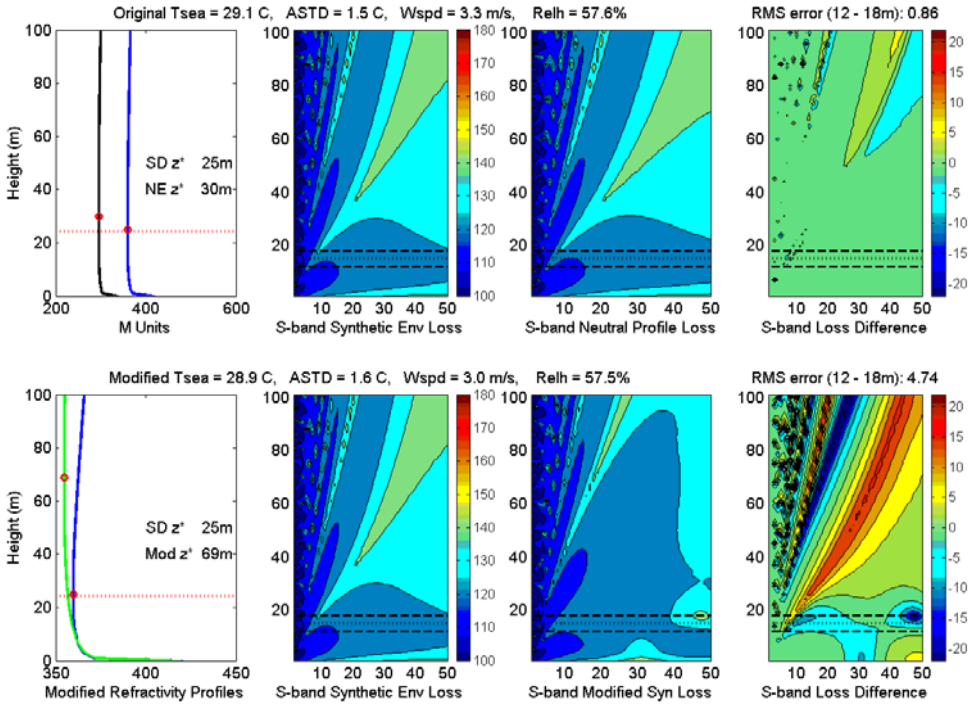

Figure 5. Stability Dependence of the Traditional Method with Measurement Errors

In contrast, the simulated RFC method does not have a clear dependence on stability. In the cases that exclude sub-refractive profiles, all of the model runs show the unstable cases as having a slightly larger error, but a smaller spread, than the stable cases. Once the sub-refractive profiles are added, even though they account for only seven percent of the cases on average, a clear stability dependence is shown with larger errors on the stable side and unchanged errors on the unstable side (nearly all (> 99%) of the sub-refractive cases are stable). What to attribute this error to is unknown. For example, could it be caused by an inadequate library of neutral profiles or is it due to the unrealistic stability dependent profiles that the RFC method is attempting to find an equivalent profile for?

B. FREQUENCY DEPENDENCE

The dependence on frequency is also obvious with most errors in the X-band two to three times as large as those in the S-band. Operationally for RFC, this simple means that caution should be taken when using an S-band derived profile to predict X-band propagation. Overall, the neutral equivalent profile can give the radar operator a good idea of the propagation effects of X-band waves but for tactical assessments, errors greater than three decibels may be too large to warrant their use.

The main reason for the increase in error is due to the shorter length (higher frequency) of the radio waves. The size of the duct (d) required to trap a given frequency (f_{min}) is given by equation (16). In order to significantly impact S-band propagation, the duct has to be at least 24.3 meters while for the X-band, the duct only has to be 11 meters. Thus many more evaporative ducting conditions exist that significantly impact X-band propagation compared to S-band propagation.

$$d_{\min} = \left(\frac{3.6 * 10^{11}}{f_{\min}} \right)^{2/3} \tag{16}$$

C. HEIGHT DEPENDENCE

Another trend displayed in the S-band RMS error is that the higher the 'height of concern', the more error there is. Since the RFC method guarantees a best fit at one meter, it is reasonable to have larger errors at heights farther away from the height at which the neutral equivalent profile was determined. What was not expected was the relative size of the increasing error in that more error was expected at higher heights simply due to the unique propagation effects (shadow zones and nodes) that occur with evaporation ducts. This result is encouraging since the actual height of an inbound anti-ship missile is normally unknown unless very accurate intelligence can determine the type of missile. Even so, there are many variants of the same missile and many times the enemy operator can choose what height the missile's terminal maneuver will use.

D. SUB-REFRACTIVE PROFILES

As expected, the inclusion of the sub-refractive profiles in the simulation increased the RMS error of the RFC method but it also increased the error of the modified stability dependent benchmark. The inclusion of these profiles did not impact the detection range errors (results not presented above), as the results with and without sub-refractive profiles were the same for each simulation run. After looking at these sub-refractive cases, there is a point at which the slope of the clutter power falloff doesn't change. A majority of the sub-refractive profiles reach this point and thus the calculated detection ranges are the same regardless of the method used to generate a refractive profile. For example, most of the sub-refractive profiles alter the standard atmosphere detection range of ten nautical miles down to two nautical miles.

THIS PAGE INTENTIONALLY LEFT BLANK

VI. CONCLUSIONS

A simulation-based analysis of the RFC method was carried out and results showed that model error is comparable to that of the traditional method with measurement errors. Excluding the sub-refractive cases, the S-band RMS error is only around one decibel and the detection ranges within five percent of the actual values (as determined by the stability dependent profile). There is some impact of height with respect to how accurate the neutral equivalent profile is but not enough to discount its use up to at least thirty meters (the highest height used in this simulation). Though the X-band errors were significantly larger than S-band errors, the neutral equivalent profile can be used to predict the general propagation of systems operating at X-band; however, some caution should be used if using the actual loss values predicted by a propagation model as the average error was slightly larger than 3 decibels.

THIS PAGE INTENTIONALLY LEFT BLANK

VII. FOLLOW-ON WORK

A. IMPROVE UPON THE CLIMATOLOGY

There are several ways that the simulation-based study could be improved to more accurately represent both the environment and the RFC method. One is to improve upon the climatology database used to generate the original datasets for the 'ground truth' stability dependent profile. Though the method used here seems adequate, using raw statistics (mean and standard deviation) tends to skew the actual observation set as a whole. For example, a simple Guassian distribution does not account for the bi-modal distribution of air-temperatures found in the Persian Gulf. Moreover, it is naïve to think that the five parameters used here are independent of each other. Only the sea surface temperature and air temperature were kept dependent on one another; the others were randomly generated. One would also expect that the sea level pressure has an impact on the magnitude of the wind speed and thus an impact on the relative humidity as well.

The point here is that a more thorough way of representing the GMCA dataset could be integrated to use whole observations as submitted to the COADS database. This would involve a very large dataset (5 parameters of over 100,000 observations each for an individual area), coded with a random number generator that chooses one set of observations from the list. This would ensure that the inter-dependence of the parameters is maintained as well as accomplishing an adequate statistical sampling of the database. This may also help alleviate the questionable sub-refractive profiles generated by the NPS-LKB model.

Another improvement would be to run the simulation in a variety of basins with significantly different climates. The three areas used in this simulation are more similar than they are different as they all are relatively shallow, warm bodies of water. Areas with more contrast that represent a larger set of the normal operating areas for the US Navy would provide a more thorough simulation (for example the Atlantic, Caribbean, Mediterranean, and Yellow Sea – all which have prolonged periods of stable conditions due to cold water sources and arguably more synoptic meteorological impacts).

B. IMPROVE THE SUB-REFRACTIVE MODEL

An alternative method of generating neutral sub-refractive profiles could be used as presented by *Livingston* (1970). Visual observations of the sub-refractive profiles indicate a good fit by RFC in the lower ten meters, but interference creates some shadow zones not properly modeled by any of the neutral sub-refractive profiles. A better model, larger neutral library or some combination thereof may improve the results.

C. IMPROVE UPON THE DETECTION RANGE ERROR METHOD

A step in this direction most likely involves a classification issue but what is most useful from a surface ship perspective is an adequate analysis of whether a system is tactically sound, not just scientifically justified. One to two decibel errors at any given height may or may not impact the actual detection range much but with the issue of ship survivability at stake, an more rigorous investigation of the tactical errors involved in RFC (or any system used to derive refractive profiles) is certainly warranted.

D. CONDUCT A FIELD EXPERIMENT

Simulations like this one are important to investigate issues without many resources and certainly lead the way to more efficient field experiments. This simulation is also useful for isolating certain errors or perceived errors of the RFC method while possibly discovering others not anticipated; but to that extent, simulations are limited in scope. A true assessment of RFC, with all of its errors, lies in a field experiment using real data and actual ship sensors and radar systems.

A simple experiment would record not only the environmental parameters to create a stability dependent profile, but also the actual clutter power produced by the radar. In this way, the RFC method could be compared against the measured stability dependent profile and predicted propagation loss matrix. This type of experiment would obvious test more than just RFC as the errors of the stability dependent model, the propagation model, the radar system and the RFC step could be cumulative (or possibly offset).

A more complex experiment would probably have to be coordinated on a higher level in order to involve a tactical approach appropriate to answering questions raised above. The use of direct refractivity sensors via a rocket-sonde or kite would certainly help provide a true benchmark to compare both methods against. (Some data similar to the proposed experiment above is already available from the 1999 operational test of RFC in conjunction with TEP onboard the USS O'KANE.)

THIS PAGE INTENTIONALLY LEFT BLANK

LIST OF REFERENCES

Anderson, K. D., 1995; Radar Detection of Low-Altitude Targets in a Maritime Environment. *IEEE Trans. Antennas Propag.*, **43**, No. 6, 609-613.

Babin, S. M., G. S. Young and J. A. Carton, 1997; A New Model of the Oceanic Evaporation Duct. *J. Appl. Meteo.*, **36**, No. 3, 193-204.

Barton, D. K., 1988; *Modern Radar System Analysis*, Artech House, Norwood, MA, 10-43.

CNO (N88, N86, N85, and N096) and NAVAIR (PMA 251), 1998; MORIAH Operational Requirements Document (ORD). (**SECRET** (US ONLY) document, **UNCLASSIFIED** upon removal of APPENDIX B).

Dockery, G. D., 1998; Development and Use of Electromagnetic Parabolic Equation Propagation Models for U.S. Navy Applications. *Johns Hopkins APL Technical Digest*, **19**, No. 3, 283-292.

Frederickson, P. A., K. L. Davidson, and A. K. Goroch, 2000; Operational Bulk Evaporation Duct Model for MORIAH. NPS Draft Report (Version 1.2).

Gerstoft, P., L. T. Rogers, J. L. Krolik and W. S. Hodgkiss, 2001; Inversion of Refractivity Parameters from Radar Sea Clutter. Submitted to *Radio Science*.

Hitney, H. V., 1994; Refractive Effects from VHF to EHF, Part B: Propagation Models. *NATO AGARD LS-196*.

Jeske, H., 1971; The State of Radar-Range Prediction Over Sea. Tropospheric Radio Wave Propagation Part II, *NATO APGARD CP-70*, Paper 50.

Jeske, H., 1973; State and Limits of Prediction Methods of Radar Wave Propagation Conditions Over Sea. *Modern Topics in Microwave Propagation and Air-Sea Interaction*, A. Zancla, ed., Reidel Publishers, 131-148.

Liu, W. T., K. B. Katsaros, and J. A. Businger, 1979; Bulk Parameterization of Air-Sea Exchanges of Heat and Water Vapor Including the Molecular Constraints at the Interface. *J. Atmos. Sci.*, **36**, 1722-1735.

Livingston, D.C., 1970; The Physics of Microwave Propagation. Prentice-Hall, 71-85.

Pappert, R. A., R. A. Paulus, and F. D. Tappert, 1992; Sea Echo in Tropospheric Ducting Environments, *Radio Sci.*, **27**, No. 2, 189-209.

Paulus, R. A., 1985; Practical Application of an Evaporation Duct Model. *Radio Sci.*, **20**, No. 4, 887-896.

Paulus, R. A. and W. K. Moision, 2001; Analysis of Evaporation Duct Height Correlation. Battlespace Atmospheric and Cloud Impacts on Military Operations Conference, Colorado State University, Fort Collins, CO.

Paulus, R. A., 1995; Proceedings of the Electromagnetic Propagation Workshop. *NOSC TD 2891*.

Paulus, R. A., 2000; Parametric Study of Propagation in Evaporation Ducting and Subrefractive Conditions. *SSC San Diego TR 1844*.

Rogers, L. T., C. P. Hattan and J. K. Stapleton, 2000; Estimating Evaporation Duct Heights from Radar Sea Echo. *Radio Science*, **35**, No. 4, 955-966.

Rogers, L. T. and R. A. Paulus, 1996; Measured Performance of Evaporation Duct Models. *Proceedings of the Battlespace Atmospherics Conference*, Tech. Doc. 2938, 273-281.

Sadanaga, D. A., 1999; Performance Evaluation of Integrated METOC Measurement System Supporting Naval Operations, MS Thesis, Naval Postgraduate School, Monterey, CA.

Space and Naval Warfare Systems Command 2000; *User's Manual (UM) for Advanced Refractive Effects Prediction System Version 2.0*, Draft, Space and Naval Warfare Systems Command, METOC Systems Program Office (SPAWAR PMW-185), San Diego, CA.

THIS PAGE INTENTIONALLY LEFT BLANK

INITIAL DISTRIBUTION LIST

1. Defense Technical Information Center
   Fort Belvoir, Virginia

2. Dudley Knox Library
   Naval Postgraduate School
   Monterey, California

3. The Oceanographer of the Navy
   Washington, DC

4. Commander
   Space and Naval Warfare Systems Command (PMW-155)
   San Diego, CA

5. Kenneth L. Davidson
   Meteorology Department, Code MR/DS
   Naval Postgraduate School
   Monterey, California

6. L. Ted Rogers
   Space and Naval Warfare Systems Center
   Propagation Division, Code D883
   San Diego, California

7. Professor C. Wash
   Meteorology Department, Code MR/WX
   Naval Postgraduate School
   Monterey, California

8. Commander
   Naval Surface Warfare Center, Dahlgren Division (NSWCDD)
   Code T44
   Dahlgren, Virginia

9. The Johns Hopkins University, Applied Physics Laboratory
   Laurel, Maryland

10. LCDR Marc C. Eckardt
    USS Abraham Lincoln, CVN-72